Procedia Computer Science
Volume 80, 2016, Pages 1093–1102
ICCS 2016. The International Conference on Computational Science

Sequential Domain Patching for Computationally Feasible Multi-Objective Optimization of Expensive Electromagnetic Simulation Models

Adrian Bekasiewicz[1,2*†], Slawomir Koziel[1,2‡§] and Leifur Leifsson[3**]
[1]*Reykjavik University, Iceland*
[2]*Gdansk University of Technology, Poland*
[3]*Iowa State University, Ames, Iowa, USA*
bekasiewicz@ru.is, koziel@ru.is, leifur@iastate.edu

Abstract
In this paper, we discuss a simple and efficient technique for multi-objective design optimization of multi-parameter microwave and antenna structures. Our method exploits a stencil-based approach for identification of the Pareto front that does not rely on population-based metaheuristic algorithms, typically used for this purpose. The optimization procedure is realized in two steps. Initially, the initial Pareto-optimal set representing the best possible trade-offs between conflicting objectives is obtained using low-fidelity representation (coarsely-discretized EM model simulations) of the structure at hand. This is realized by sequential construction and relocation of small design space segments (patches) in order to create a path connecting the extreme Pareto front designs identified beforehand. In the second step, the Pareto set is refined to yield the optimal designs at the level of the high-fidelity electromagnetic (EM) model. The appropriate number of patches is determined automatically. The approach is validated by means of two multi-parameter design examples: a compact impedance transformer, and an ultra-wideband monopole antenna. Superiority of the patching method over the state-of-the-art multi-objective optimization techniques is demonstrated in terms of the computational cost of the design process.

Keywords: multi-objective optimization, sequential domain patching, surrogate modeling, antenna design, impedance transformer design

* Engineering Optimization & Modeling Center, School of Science and Engineering
† Faculty of Electronics, Telecommunications and Informatics
‡ Engineering Optimization & Modeling Center, School of Science and Engineering
§ Faculty of Electronics, Telecommunications and Informatics
** Department of Aerospace Engineering, Iowa State University

doi:10.1016/j.procs.2016.05.414

1 Introduction

Design of contemporary microwave and antenna components is a challenging process that involves adjustment of geometrical parameters of the structures so that given performance requirements are satisfied. Modern structures are often characterized by complex and multi-parameter geometries with non-intuitive relations between dimensions and the performance characteristics. Therefore, conventional design approaches based on repetitive parameter sweeps (mostly one parameter at a time) guided by engineering experience turn to be inefficient and unable to yield truly optimum solutions. For that reason, automated determination of the optimum structure dimensions by means of numerical optimization techniques is highly desirable yet quite challenging. The main obstacle is that—in most cases—performance characteristics of modern microwave and antenna structures can be accurately evaluated only by means of high-fidelity electromagnetic (EM) simulations. At the same time, numerical optimization using both local (e.g., gradient-based (Nocedal and Wright, 2006)) methods as well as global ones (e.g., evolutionary algorithms (Kuwahara, 2005)) involves hundreds, thousands or even tens of thousands of model evaluations. Consequently, application of such algorithms is computationally prohibitive if expensive EM simulation models are utilized for performance evaluation of the structures under design.

In many situations, design of real-life microwave and antenna structures requires simultaneous handling of several, often conflicting, design requirements such as minimization of return loss within the frequency band of interest, reduction of the power split error, or maximization of gain (Koziel and Ogurtsov, 2013). There may be also objectives related to the structure geometry, e.g., reduction of its size or volume (Koziel and Ogurtsov, 2013). Obtaining comprehensive data concerning the best possible trade-offs between such figures (a so-called Pareto front) is often indispensable for making application-dependent design decisions (Deb 2001). Population-based metaheuristics (evolutionary algorithms (Deb, 2001), particle swarm optimizers (Afshinmanesh, Marandi and Shahabadi, 2008), etc.) belong to the most popular solution approaches for solving design tasks with multiple design requirements. Although the mentioned techniques allow for yielding the entire representation of the Pareto front in one algorithm run, they are not practical for solving real-world design problems that involve computationally expensive EM models. The reason is their tremendous CPU cost (Bekasiewicz and Koziel, 2015).

The difficulties related to high computational cost of multi-objective optimization can be partially alleviated by means of surrogate-based optimization (SBO) techniques. SBO allows for shifting the optimization burden to a fast yet less accurate representation of the structure at hand (a so-called surrogate model). The latter is normally constructed from coarsely discretized EM simulation model or equivalent network models in case of certain microwave structures (such as filters). Surrogate-based techniques have been successfully utilized for solving multi-objective design problems. For instance, in (Koziel and Ogurtsov, 2013) a response surface approximation (RSA) model obtained from coarsely-discretized simulation data has been utilized along with a multi-objective evolutionary algorithm (MOEA) to yield an initial approximation of the Pareto front. The final Pareto front has been generated using sufficient response correction technique. In (Koziel et al., 2014), co-kriging surrogates have been exploited to improve the quality of the MOEA-based Pareto front by incorporating high-fidelity model data to the RSA. Moreover, applicability of these techniques has been extended to multi-parameter design problems by using design space reduction techniques (Koziel, Bekasiewicz and Zieniutycz, 2014).

Despite advancements in expedited multi-objective optimization, a common weakness of the aforementioned techniques is the necessity of using population-based metaheuristics for identification of the Pareto front. Moreover, these techniques require a rather careful allocation of the designn space subset containing the optimum designs (Koziel, Bekasiewicz and Zieniutycz, 2014). Additionally, construction of the fast approximation models required in mentioned works is subject to various limitations, particularly the curse of dimensionality (exponential growth of the necessary number of training data samples with the number of antenna geometry parameters) (Forrester and Keane, 2009). In order to address these difficulties, a multi-objective optimization technique that does not require population-based metaheuristic algorithms for identification of the Pareto set has been proposed in (Koziel, Bekasiewicz and Leifsson, 2015). The technique generates an initial approximation of the Pareto front by means of a stencil-based sequential patching of the design space sub-region limited by the extreme Pareto optimal solutions obtained using design space reduction techniques (Koziel, Bekasiewicz and Zieniutycz, 2014). The path between the extreme designs consists of a predetermined number of patches (intervals in n-dimensional design space). The patching process is executed at the level of coarse-discretization EM model, whereas the final representation of the Pareto front is obtained using response correction methods and local approximation surrogates.

In this work, we demonstrate applicability of the sequential domain patching (SDP) technique for numerically demanding design problems with multiple adjustable parameters. The original SDP algorithm is supplemented with a mechanism that automatically determines the size of the patch based on sensitivity analysis. Two design cases are used for illustration: a compact ultra-wideband (UWB) 50-to-130 Ohm microstrip impedance transformer with 15 design parameters and a 13-variable ultra-wideband monopole antenna.

2 Multi-Objective Optimization Using Domain Patching

In this section, we describe the multi-objective problem and provide details of the sequential domain patching procedure. We also describe the algorithm for automated determination of patch size and briefly discuss the technique for refinement of the selected Pareto-optimal designs.

2.1 Multi-Objective Problem Formulation

Let $\boldsymbol{R}_f(\boldsymbol{x})$ be a response of the high-fidelity EM model of the structure under design, where $\boldsymbol{x}$ is a vector of designable parameters. Then, let $F_k(\boldsymbol{x})$, $k = 1, \ldots, N_{obj}$, be a k-th design objective. If $N_{obj} > 1$ then any two designs $\boldsymbol{x}^{(1)}$ and $\boldsymbol{x}^{(2)}$ for which $F_k(\boldsymbol{x}^{(1)}) < F_k(\boldsymbol{x}^{(2)})$ and $F_l(\boldsymbol{x}^{(2)}) < F_l(\boldsymbol{x}^{(1)})$ for at least one pair $k \neq l$, are not commensurable, i.e., none is better than the other in the multi-objective sense. In this case, a Pareto dominance relation $\prec$ is utilized (Deb, 2001). We say, for any two designs $\boldsymbol{x}$ and $\boldsymbol{y}$, that $\boldsymbol{x}$ dominates over $\boldsymbol{y}$ ($\boldsymbol{x} \prec \boldsymbol{y}$) if $F_k(\boldsymbol{x}) \leq F_k(\boldsymbol{y})$ for all $k = 1, \ldots, N_{obj}$, and $F_k(\boldsymbol{x}) < F_k(\boldsymbol{y})$ for all at least one k. A goal of multi-objective optimization is to find a representation of a so-called Pareto optimal set X_P composed of the non-dominated designs from the solution space X, such that for any $\boldsymbol{x} \in X_P$, there is no $\boldsymbol{y} \in X$ for which $\boldsymbol{y} \prec \boldsymbol{x}$ (Deb, 2001).

2.2 Design Space Reduction

The aim of the design space reduction procedure is to narrow the ranges of the structure parameters to the region consisting the Pareto-optimal designs. The procedure can be formulated as follows (Koziel, Bekasiewicz and Zieniutycz, 2014). Let $\boldsymbol{l}$ and $\boldsymbol{u}$ be the arbitrarily defined lower/upper bounds of the solution space. Let

$$\boldsymbol{x}_k^* = \arg\min_{\boldsymbol{l} \leq \boldsymbol{x} \leq \boldsymbol{u}} F_k\left(\boldsymbol{R}_c(\boldsymbol{x})\right) \tag{1}$$

where $k = 1, \ldots, N_{obj}$ be an optimum design of the low-fidelity model $\boldsymbol{R}_c$ obtained with respect to the kth objective. The designs $\boldsymbol{x}_c^{*(k)}$ are found for all of the considered objectives, one at a time.

The numerical cost of solving (1) depends on the dimensionality of the design problem. Typically, it corresponds to about a hundred to a few hundreds of the low-fidelity model evaluations. Once the “extreme” Pareto optimal designs are identified, the sequential domain patching algorithm can be executed to approximate Pareto front.

2.3 Sequential Domain Patching Algorithm

The initial Pareto-optimal set is obtained by means of the SDP method. The process exploits the "extreme" designs obtained using (1). The conceptual illustration of the algorithm is shown in Fig. 1. The procedure assumes two-objective setup. The SDP algorithm works as follows (Koziel, Bekasiewicz and Leifsson, 2015):

1. Execute the algorithm of Section 2.4 to automatically determine size of the patch $\boldsymbol{d} = [d_1 \ldots d_n]^T$, where n is the number of structure adjustable parameters;
2. Set the current points $\boldsymbol{x}_{c1} = \boldsymbol{x}_1^*$ and $\boldsymbol{x}_{c2} = \boldsymbol{x}_2^*$;
3. Evaluate n perturbations of the size $\boldsymbol{d}$ around $\boldsymbol{x}_{c1}^*$ (towards $\boldsymbol{x}_{c2}^*$ only) and select the one which leads to the best improvement w.r.t. the objective F_2;
4. Relocate the patch so that its center is at the best perturbation selected in Step 3; update $\boldsymbol{x}_{c1}$;
5. Evaluate n perturbations of the size $\boldsymbol{d}$ around $\boldsymbol{x}_{c2}^*$ (towards $\boldsymbol{x}_{c1}^*$ only) and select the one which leads to the best improvement w.r.t. the objective F_1.
6. Relocate the patch so that its center is at the best perturbation selected in Step 5 and update $\boldsymbol{x}_{c2}$;
7. If the path between $\boldsymbol{x}_1^*$ and $\boldsymbol{x}_2^*$ is not complete, go to 3;

The SDP algorithm yields the initial approximation of the Pareto-optimal designs, as well as a set of boxes within the initially defined design space that cover these solutions (see Fig. 1). The numerical cost of the algorithm depends only on the dimensionality of the problem at hand and on the number of patches. It can be estimated from above (excluding the cost of solving (1)) as $(M - 1)\cdot(n - 1)$, where $M = \sum_{j = 1,\ldots,n} m_j$, and is m_j the number of intervals in the direction j computed using procedure of Section 2.4. In practice, the cost is lower since some of the necessary perturbations have been already evaluated while considering previous patches or do not need to be evaluated due to the problem constraints.

2.4 Automated Determination of Patch Sizes

Selection of the appropriate patch size is important from the algorithm efficiency standpoint. Generally, the distance between the "extreme" Pareto designs $\boldsymbol{x}_1^*$ and $\boldsymbol{x}_2^*$ in each dimension j have to be divided into the integer number of intervals denoted as m_j so that the norm-wise change of the structure responses is similar when executing patch-size perturbations. Here, we use the notation $\boldsymbol{x}_1^* = [x_{1.1}^* \ldots x_{1.n}^*]^T$ (similarly for $\boldsymbol{x}_2^*$).

The vector of intervals M is obtained as follows:

1. Evaluate $\boldsymbol{R}_c$ at n points $\boldsymbol{x}_{1\text{-}2}^{(j)} = [x_{1.1}^* \ldots x_{1.j-1}^* \; x_{2.j}^* \; x_{1.j+1}^* \ldots x_{1.n}^*]^T$ and calculate $E_{1.j} = \|\boldsymbol{R}_c(\boldsymbol{x}_{1\text{-}2}^{(j)}) - \boldsymbol{R}_c(\boldsymbol{x}_1^*)\|/\|\boldsymbol{R}_c(\boldsymbol{x}_1^*)\|$;
2. Evaluate $\boldsymbol{R}_c$ at n points $\boldsymbol{x}_{2\text{-}1}^{(j)} = [x_{2.1}^* \ldots x_{2.j-1}^* \; x_{1.j}^* \; x_{2.j+1}^* \ldots x_{2.n}^*]^T$ and calculate $E_{2.j} = \|\boldsymbol{R}_c(\boldsymbol{x}_{2\text{-}1}^{(j)}) - \boldsymbol{R}_c(\boldsymbol{x}_2^*)\|/\|\boldsymbol{R}_c(\boldsymbol{x}_2^*)\|$;
3. Set $E_j = (E_{1.j} + E_{2.j})/2$;
4. Normalize $E_j = E_j/\max\{E_j: j = 1,...,n\}$;
5. Set $m_j = \max\{2,\lceil m_{\max}\cdot E_j\rceil\}$.

The coefficients $E_{1.j}$ represent the relative changes of the structure responses for the variation of the jth component of the design $\boldsymbol{x}_1^*$ towards $\boldsymbol{x}_2^*$ (similarly for $E_{2.j}$), whereas E_j are their average values. They can be utilized to estimate the variations of structure responses between the "extreme" Pareto designs along each dimensions. The minimum number of intervals is 2 whereas the maximum m_{max} is defined by the user. The other (intermediate) values are determined as integers proportional to E_j. It should be noted that m_{max} can be estimated as follows: $m_{\max} = \lceil \max\{E_k: k = 1,\ldots,n\}/E_{\max} \rceil$ (calculated for non-normalized E_j coefficients). The value can be also approximated with respect to the assumed computational budget of the SDP given in Section 2.3.

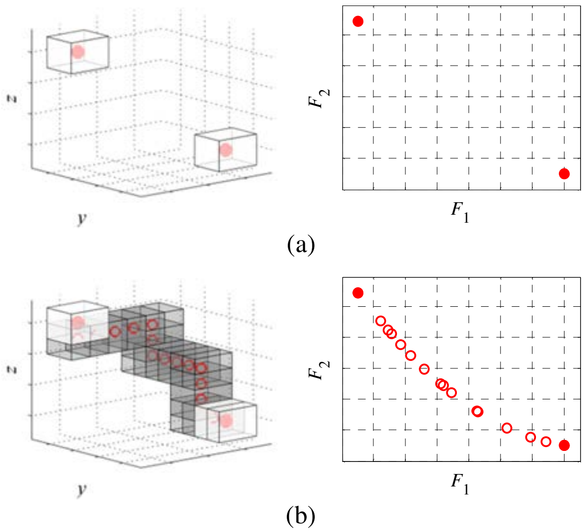

Fig. 1. A conceptual illustration of SDP algorithm (n = 3): (a) “extreme” Pareto designs obtained from (1) (●); (b) SDP-based Pareto-optimal solutions (○). Left- and right-hand side figures represent path in the design space and the feature space, respectively.

2.5 Initial Pareto Set Refinement

The Pareto set generated by the SDP algorithm (cf. Section 2.3) is obtained using the coarse-discretization model $\boldsymbol{R}_c$ and thus it has to be elevated to the $\boldsymbol{R}_f$ model level to obtain the final Pareto set. The latter can be obtained for the selected designs $\boldsymbol{x}_c^{(k)}$ (k = 1, …, K) using the following output space mapping procedure:

$$\boldsymbol{x}_f^{(k)} \leftarrow \arg \min_{\boldsymbol{x},\, F_2(\boldsymbol{x}) \le F_2(\boldsymbol{x}_f^{(k)})} F_1\left(\boldsymbol{R}_s(\boldsymbol{x}) + d\boldsymbol{R}^{(k)}\right) \tag{2}$$

where $d\boldsymbol{R}^{(k)} = \boldsymbol{R}_f(\boldsymbol{x}_f^{(k)}) - \boldsymbol{R}_s(\boldsymbol{x}_f^{(k)})$. The refinement process is aimed at improving the first objective without degrading the second one. The starting point for (2) is $\boldsymbol{x}_f^{(k)} = \boldsymbol{x}_c^{(k)}$ and the process is iterated until convergence (typically obtained within two or three iterations). The correction term $d\boldsymbol{R}^{(k)}$ ensures zero-order consistency (i.e., $\boldsymbol{R}_s(\boldsymbol{x}_f^{(k)}) = \boldsymbol{R}_f(\boldsymbol{x}_f^{(k)})$) at the beginning of each iteration (Koziel and Ogurtsov, 2013). The surrogate model $\boldsymbol{R}_s$ is constructed as a simplified second-order polynomial approximation (without mixed terms) of the $\boldsymbol{R}_c$ model at $2n + 1$ perturbed designs around $\boldsymbol{x}_c^{(k)}$ obtained using a star-distribution design of experiments. The perturbation size corresponds to patch size determined using the algorithm of Section 2.4. Note that at last half of the necessary data is already available from the patching process (cf. Section 2.3).

3 Demonstration Examples

In this section, we present numerical verification of the SDP method. Its operation is demonstrated using a 15-variable compact microstrip impedance transformer and a 13-parameter planar ultra-wideband (UWB) monopole antenna. Both structures operate within UWB frequency range. Comparison with benchmark multi-objective optimization algorithms is also provided.

3.1 Miniaturized Impedance Transformer

Our first example is a compact 50-to-130 Ohm impedance transformer shown in Fig. 2. The circuit is constructed as a cascade of three compact microstrip resonant cells (Kurgan, Bekasiewicz, and Kitlinski, 2015). It is implemented on a 0.762 mm thick Taconic RF-35 dielectric substrate (ε_r = 3.5; $tan\delta$ = 0.0018). Design variables are: $\boldsymbol{x} = [w_{11}\ w_{21}\ w_{31}\ l_{21}\ l_{31}\ w_{12}\ w_{22}\ w_{32}\ l_{22}\ l_{32}\ w_{13}\ w_{23}\ w_{33}\ l_{23}\ l_{33}]^T$, whereas w_{i1} = 1.7, w_{i2} = 0.17 and l_0 = 1. The unit for all dimensions is mm. The ranges of adjustable parameters are limited by the following lower/upper bounds are: $\boldsymbol{l}$ = [0.15 0.15 0.15 0.5 0.15 0.15 0.15 0.15 0.5 0.15 0.15 0.15 0.15 0.5 0.15]^T and $\boldsymbol{u}$ = [1 1 1 5 0.5 1 1 1 5 0.5 1 1 1 5 0.5]^T.

The transformer models are implemented in CST Microwave Studio and simulated using its time domain solver (CST, 2013). The high-fidelity model $\boldsymbol{R}_f(\boldsymbol{x})$ consists of about 1,200,000 hexahedral mesh cells and its average simulation time on a dual Intel Xeon E5540 machine is 12 min. The low-fidelity model $\boldsymbol{R}_c(\boldsymbol{x})$ contains ~120,000 cells (typical simulation time 49 s). Two design objectives are considered: minimization of maximal transformer in-band return loss defined as $F_1(\boldsymbol{x}) = \max(|S_{11}|_{2\text{ GHz to }5.5\text{ GHz}})$ and reduction of structure area defined as $F_2(\boldsymbol{x}) = A \times B$, where $A = 2\cdot(l_{21}+ l_{31}) + w_{21} + w_{12} + 2\cdot(l_{22} + l_{32}) + w_{22} + w_{13} + 2\cdot(l_{23} + l_{33}) + w_{23}$ and $B = w_{11} + w_{31} + l_{31}$. It should be noted that only designs for which satisfies requirement $F_1(\boldsymbol{x}) \leq -10$ dB are of interest.

The "extreme" Pareto-optimal designs $\boldsymbol{x}_1^*$ = [0.39 0.89 1.66 0.44 0.15 0.21 2.33 0.15 0.16 0.15 2.32 0.15]^T and $\boldsymbol{x}_2^*$ = [0.24 0.49 0.86 0.36 0.16 0.25 1.73 0.15 0.17 0.20 1.80 0.15]^T have been obtained using design space reduction procedure of Section 2.2. Note that the dimensionality of the problem has been reduced to 12 variables, in particular, the parameters w_{21} = 0.15, l_{31} = 0.15 and w_{33} = 0.15 are fixed. Subsequently, the vector of intervals M = [15 16 16 10 2 7 14 2 2 2 13 2] has been obtained using the procedure of Section 2.4. The initial representation of the Pareto front shown in Fig. 3 has been identified by means of the SDP algorithm of Section 2.3. Finally, a set of 10 designs has been selected along the Pareto front and refined to the high-fidelity model level. The obtained results (see Fig. 3) indicate that transformer responses vary by 5.3 dB and 9.2 mm^2 (over 40 percent) along Pareto front for objective $F_1(\boldsymbol{x})$ and $F_2(\boldsymbol{x})$, respectively. The geometrical details of selected high-fidelity Pareto-optimal designs are gathered in Table 1, whereas their corresponding frequency responses are shown in Fig. 4(b).

The cost of multi-objective optimization of the transformer includes: 520, 12 and 587 $\boldsymbol{R}_c$ simulations for determination of the "extreme" Pareto designs, calculation of the patching intervals and optimization using SDP algorithm, respectively, as well as 250 $\boldsymbol{R}_c$ and 30 $\boldsymbol{R}_f$ evaluations for the designs refinement.

The algorithm has been compared with two benchmark techniques based on multi-objective evolutionary algorithm (MOEA). The first method is based on utilization of response surface approximation model constructed using $\boldsymbol{R}_c$ data obtained within the region of the solution space limited by the "extreme" Pareto designs (Koziel, Bekasiewicz and Zieniutycz, 2014). The algorithm setup is: 500 individuals and 50 generations. The second method directly exploits the $\boldsymbol{R}_c$ model of the transformer for MOEA optimization (setup: 100 individuals, 100 iterations). It should be noted that utilization of the low-fidelity models is necessary because the estimated cost of direct MOEA optimization of $\boldsymbol{R}_f$ transformer model (10000 simulations) is over 83 days. The comparison of the methods has been performed under the assumption that the "extreme" Pareto designs are known. The results shown in Fig. 5 indicate that initial SDP-based front approximation is slightly dominated.

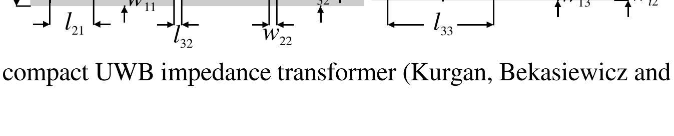

Fig. 2. Geometry of a compact UWB impedance transformer (Kurgan, Bekasiewicz and Kitlinski, 2015).

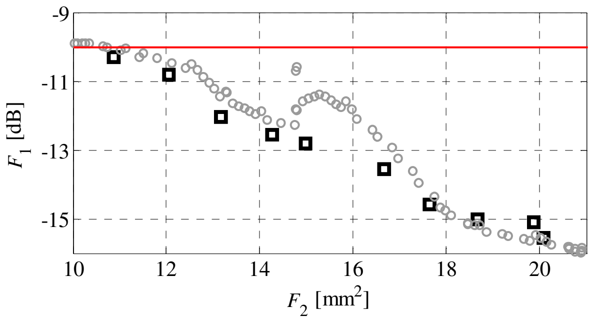

Fig. 3. The low- (○) and high-fidelity (□) designs obtained using sequential domain patching.

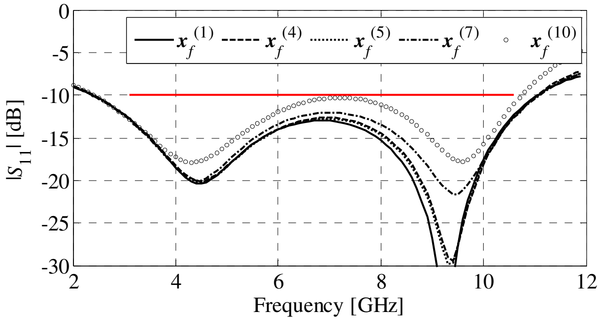

Fig. 4. Frequency characteristics of the transformer designs of Table 1.

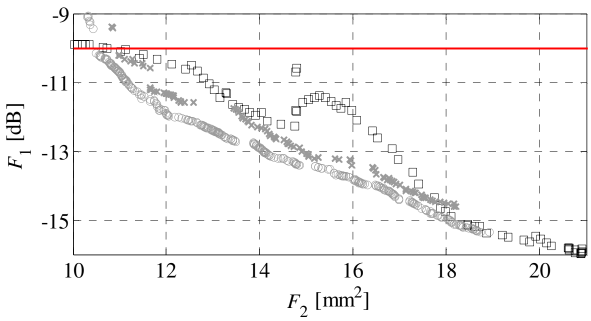

Fig. 5. Comparison of initial Pareto fronts obtained using SDP (○), as well as first (□) and second (×) benchmark method.

Table 1: Compact Impedance Transformer – Optimization Results

	F_1 [dB]	F_2 [mm^2]	Design variables											
			w_{11}	w_{31}	l_{21}	w_{12}	w_{22}	w_{32}	l_{22}	l_{32}	w_{13}	w_{23}	l_{23}	l_{33}
$x_f^{(1)}$	–15.6	20	0.41	0.85	1.73	0.41	0.16	0.22	2.24	0.15	0.16	0.16	2.17	0.15
$x_f^{(4)}$	–14.6	18	0.42	0.74	1.66	0.35	0.16	0.24	2.04	0.16	0.15	0.16	2.08	0.16
$x_f^{(5)}$	–13.6	17	0.41	0.69	1.64	0.37	0.16	0.24	2.01	0.16	0.16	0.16	2.09	0.16
$x_f^{(7)}$	–12.5	14	0.40	0.64	1.20	0.37	0.16	0.23	1.75	0.16	0.16	0.16	2.09	0.16
$x_f^{(10)}$	–10.3	11	0.29	0.50	0.87	0.40	0.16	0.20	1.74	0.17	0.15	0.16	2.18	0.17

The computational cost of multi-objective design optimization using the benchmark techniques corresponds to about 68 and 681 $\boldsymbol{R}_f$ model simulations for the first and the second benchmark technique, respectively. At the same time, the cost of SDP is about 41 $\boldsymbol{R}_f$ which is 40% and 94% lower compared to MOEA-based methods.

3.2 Planar Monopole Antenna

The second example is an UWB monopole shown in Fig. 6 (Koziel, Bekasiewicz and Zieniutycz, 2014). The structure consists of a driven element in the form of three stacked trapezoids fed through a 50 Ohm microstrip line and it is designed on a 0.762 mm thick Taconic RF-35 substrate. Design parameters are: $\boldsymbol{x} = [a_1\ a_2\ a_3\ a_4\ a_5\ a_6\ b_1\ b_2\ b_3\ w_2\ l\ d\ o]^T$. whereas $w_1 = 1.7$ to ensure 50 Ohm input impedance (all dimensions are in mm). The initial design bounds are: $\boldsymbol{l} = [5\ 5\ 5\ 5\ 5\ 5\ 1\ 1\ 1\ 0.2\ 8\ 20\ 5]^T$ and $\boldsymbol{u} = [25\ 25\ 25\ 25\ 25\ 25\ 15\ 15\ 15\ 2\ 15\ 40\ 10]^T$.

The high-fidelity model (2,500,000 mesh cells, simulation time: 10 min) and the low-fidelity one (~33,600 cells, simulation time 22 s) are both implemented in CTS Microwave Studio.. Design objectives are: F_1 – minimization of the antenna reflection within 3.1 GHz to 10.6 GHz frequency and F_2 – reduction of the size defined by $A \times B$ rectangle, where $A = l + d + b_1 + b_2 + b_3 + o$ and $B = w_2 + o$.

The "extreme" Pareto designs are: $\boldsymbol{x}_1^* = [10.07\ 21.63\ 22.2\ 21\ 20.8\ 22.7\ 3.9\ 3.8\ 12.32\ 0.6\ 11.15\ 28.34\ 5]^T$ and $\boldsymbol{x}_2^* = [10.97\ 21.76\ 22.2\ 22.79\ 21.01\ 23.7\ 3.9\ 3.92\ 13.02\ 0.67\ 10.6\ 35.35\ 5]^T$. The vector of intervals is $M = [4\ 3\ 2\ 4\ 3\ 3\ 3\ 3\ 2\ 4\ 5\ 3\ 15\ 3]$. The initial representation of the Pareto front obtained using the SDP algorithm and ten designs evenly distributed along the Pareto front are shown in Fig. 7. Based on the obtained results one can conclude that the antenna responses w.r.t. objective F_1 and F_2 vary by 4.6 dB and 308 mm^2 (almost 22 percent), respectively. The antenna frequency responses for the selected designs from Table 2 are shown in Fig. 8. The cost of multi-objective antenna optimization includes 800, 13 and 248 $\boldsymbol{R}_c$ simulations for determination of "extreme" Pareto designs, determination of the vector of intervals and SDP optimization, respectively. Refinement of the selected designs required 270 $\boldsymbol{R}_c$ and 30 $\boldsymbol{R}_f$ model evaluations.

The algorithm has been compared with two MOEA-based optimization techniques. The first method exploits the RSA model constructed using $\boldsymbol{R}_c$ data acquired within the part of the solution space defined by the "extreme" designs (setup: 500 individuals and 50 generations). In the second method, MOEA optimization is performed directly on the $\boldsymbol{R}_c$ model (setup: 100 individuals, 100 iterations). Similarly as in Section 3.1, the comparison has been performed using the low-fidelity model because direct optimization of the high-fidelity model would be prohibitively expensive. The results shown in Fig. 9 indicate that SDP-based front is similar to the MOEA-based ones.

The computational cost of multi-objective design optimization using the benchmark techniques (excluding single-objective optimizations run to find the "extreme" designs) corresponds to 58, 367 $\boldsymbol{R}_f$ simulations for the first and second MOEA-based method. The cost of SDP is ~9 $\boldsymbol{R}_f$ which is 84% and 98% lower compared to the MOEA-based optimization methods.

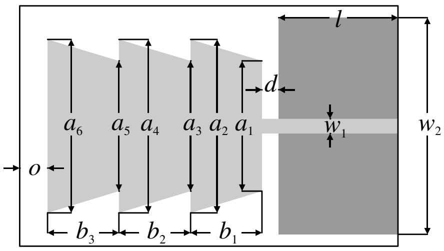

Fig. 6. Geometry of the considered monopole antenna (Koziel, Bekasiewicz and Zieniutycz, 2014).

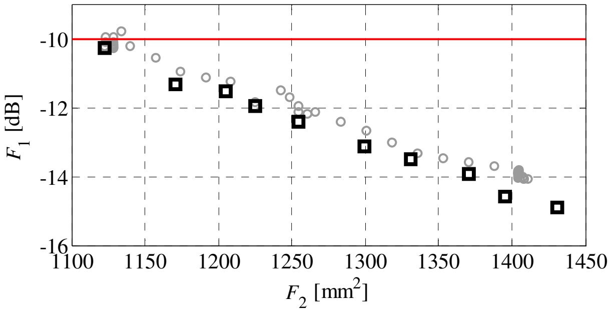

Fig. 7. The low- (○) and high-fidelity (□) designs obtained using sequential domain patching.

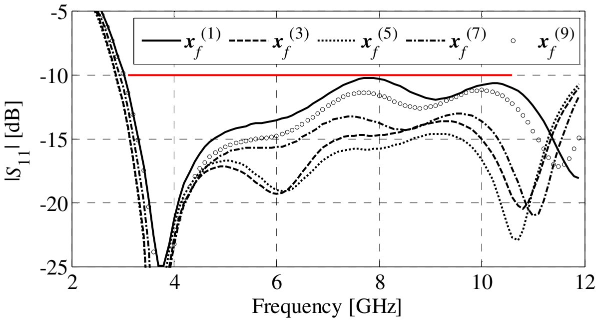

Fig. 8. Frequency characteristics of transformer designs of Table 2.

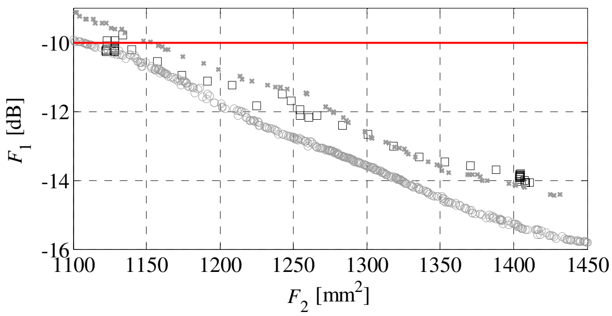

Fig. 9. Comparison of initial Pareto fronts obtained using SDP (□), as well as first (○) and second (×) benchmark method.

Table 2: UWB Monopole Antenna – Optimization Results

	F_1 [dB]	F_2 [mm^2]	Design variables												
			a_1	a_2	a_3	a_4	a_5	a_6	b_1	b_2	b_3	w_2	l	d	o
$x_f^{(1)}$	-10.3	1123	10.7	21.63	22.20	21.0	20.94	23.70	3.9	3.8	12.32	0.60	10.79	28.34	5.00
$x_f^{(4)}$	-11.5	1205	11.2	21.60	22.20	21.5	21.01	23.81	3.9	3.8	12.42	0.60	10.61	30.68	5.00
$x_f^{(5)}$	-12.4	1254	11.4	21.63	22.20	21.9	20.94	23.70	3.9	3.8	12.67	0.62	10.79	31.61	5.00
$x_f^{(7)}$	-13.5	1331	10.8	21.64	22.20	21.7	20.97	23.77	3.9	3.8	13.12	0.61	10.70	33.34	5.00
$x_f^{(10)}$	-14.6	1395	11.0	21.59	22.20	21.5	21.01	24.00	3.9	3.9	13.19	0.60	10.81	34.85	5.00

4 Conclusion

In this work a sequential-domain patching algorithm with automated determination of the patch sizes has been discussed. The method exploits variable-fidelity EM simulation models and allows for unattended expedited multi-objective optimization of microwave and antenna structures without the necessity of exploiting population-based metaheuristic algorithms. Our method has been compared to the state-of-the-art methods based on multi-objective evolutionary algorithms and proved its superiority in terms of computational cost and, in some cases, the quality of the obtained Pareto fronts. Our further work will focus on experimental verification of the obtained designs. Moreover, extension of the sequential domain patching algorithm to handle structures with more complex responses such as microwave couplers, or narrow band antennas will also be considered.

Acknowledgement

The authors would like to thank Computer Simulation Technology AG, Darmstadt, Germany, for making CST Microwave Studio available. This work has been partially supported by the Icelandic Centre for Research (RANNIS) Grant 141272051 and by National Science Center, Poland under grants 2013/11/B/ST7/04325 and 2014/12/T/ST7/00045.

References

Afshinmanesh, F., Marandi, A., Shahabadi, M. (2008) *Design of a Single-Feed Dual-Band Dual-Polarized Printed Microstrip Antenna Using a Boolean Particle Swarm Optimization*. IEEE Trans. Antennas Prop., 56, 1845-1852.

Bekasiewicz, A., Koziel, S. (2015) “Structure and Computationally-Efficient Simulation-Driven Design of Compact UWB Monopole Antenna,” *IEEE Ant. Wireless Prop. Lett.*, vol. 14, pp. 1282-1285.

CST Microwave Studio, ver. 2012, CST AG, Bad Nauheimer Str. 19, D-64289 Darmstadt, Germany, 2012.

Deb., K. (2001) *Multi-Objective Optimization Using Evolutionary Algorithms*. John Wiley & Sons.

Forrester, A.I.J., Keane, A.J. (2009) *Recent advances in surrogate-based optimization*. Prog. Aerospace Sci., 45, 50-79.

Koziel, S., Ogurtsov, S. (2013) *Multi-Objective Design of Antennas Using Variable-Fidelity Simulations and Surrogate Models*. IEEE Trans. Antennas Prop. 61, pp. 5931-5939.

Koziel, S., Bekasiewicz, A., Zieniutycz, W. (2014) *Expedite EM-Driven Multi-Objective Antenna Design in Highly-Dimensional Parameter Spaces*. IEEE Antennas Wireless Prop. Lett., 13, 631-634.

Koziel, S., Bekasiewicz, A., Couckuyt, I., Dhaene, T. (2014) *Efficient Multi-Objective Simulation-Driven Antenna Design Using Co-Kriging*. IEEE Trans. Antennas Prop. 62, 5900-5905.

Koziel, S., Bekasiewicz, A., Leifsson, L. (2015) *Rapid EM-driven antenna dimension scaling through inverse modeling*., IEEE Ant. Wireless Prop. Lett., 2015.

Kurgan, P., Bekasiewicz, A., Kitlinski, M. (2015) *On the low-cost design of abbreviated multi-section planar matching transformer*. *Microwave Opt. Techn. Lett.*, 57, 521-525.

Kuwahara, Y. (2005) *Multiobjective optimization design of Yagi-Uda antenna*. IEEE Trans. Antennas Prop., 53, 1984-1992.

Nocedal, J., Wright, S. (2006) *Numerical Optimization*, 2nd edition, Springer, New York.